Immunity, Volume *54*

Supplemental information

Immunizations with diverse sarbecovirus receptor-binding domains elicit SARS-CoV-2 neutralizing antibodies against a conserved site of vulnerability

Deborah L. Burnett, Katherine J.L. Jackson, David B. Langley, Anupriya Aggarwal, Alberto Ospina Stella, Matt D. Johansen, Harikrishnan Balachandran, Helen Lenthall, Romain Rouet, Gregory Walker, Bernadette M. Saunders, Mandeep Singh, Hui Li, Jake Y. Henry, Jennifer Jackson, Alastair G. Stewart, Franka Witthauer, Matthew A. Spence, Nicole G. Hansbro, Colin Jackson, Peter Schofield, Claire Milthorpe, Marianne Martinello, Sebastian R. Schulz, Edith Roth, Anthony Kelleher, Sean Emery, Warwick J. Britton, William D. Rawlinson, Rudolfo Karl, Simon Schäfer, Thomas H. Winkler, Robert Brink, Rowena A. Bull, Philip M. Hansbro, Hans-Martin Jäck, Stuart Turville, Daniel Christ, and Christopher C. Goodnow

Supplementary Materials for:

Immunization to elicit SARS-CoV-2 neutralizing antibodies against a conserved vulnerability of the receptor binding domain

Authors:

Deborah L. Burnett[1,2*], Katherine J. L. Jackson[1,], David B. Langley[1], Anupria Aggrawal[3], Alberto Ospina Stella[3], Matt D. Johansen[4], Harikrishnan Balachandran[3], Helen Lenthall[1], Romain Rouet[1,2], Gregory Walker[2], Bernadette M. Saunders[4], Mandeep Singh[1,2], Hui Li[3], Jake Y. Henry[1], Jennifer Jackson[1], Alastair G. Stewart[2,5], Franka Witthauer[7], Matthew A. Spence[8], Nicole G. Hansbro[4], Colin Jackson[8], Peter Schofield[1,2], Claire Milthorpe[1], Marianne Martinello[3], Sebastian R. Schulz[7], Edith Roth[7], Anthony Kelleher[3], Sean Emery[3], Warwick J. Britton[10], William D. Rawlinson[2,6], Rudolfo Karl[9], Simon Schäfer[9], Thomas H. Winkler[9], Robert Brink[1,2], Rowena A. Bull[2,3], Philip M. Hansbro[4], Hans-Martin Jäck[7], Stuart Turville[2,3], Daniel Christ[1,2]†, Christopher C. Goodnow[1,11]†.

Affiliations:

1. Garvan Institute of Medical Research, Sydney, NSW, Australia, 2010.
2. UNSW Sydney, Faculty of Medicine, Sydney, NSW, Australia, 2010.
3. Kirby Institute, UNSW, Sydney, NSW, Australia, 2052.
4. Center for Inflammation, Centenary Institute and University of Technology Sydney, Faculty of Science, School of Life Sciences, Sydney, NSW, Australia, 2006.
5. Victor Chang Cardiac Research Institute, Sydney, NSW, Australia 2010.
6. Serology and Virology Division (SAViD), NSW Health Pathology, SEALS Randwick, Sydney, NSW, Australia, 2031.
7. Division of Molecular Immunology, University Hospital Erlangen, University of Erlangen-Nürnberg, Erlangen, Germany, 91054.
8. Research School of Chemistry, Australian National University, Canberra, ACT, Australia, 2601.
9. Division of Genetics, Department Biology, Friedrich-Alexander-University Erlangen-Nürnberg (FAU), Erlangen, Germany 91054.
10. Centenary Institute, The University of Sydney, Sydney. NSW Australia, 2006
11. Cellular Genomics Futures Institute, UNSW Sydney, NSW, Australia 2052

†=Joint senior authors;

* Correspondence to d.burnett@garvan.org.au.

This PDF file includes:

Figs. S1 to S6

Captions for tables S1 to S3.

Table S4.

Other Supplementary Materials for this manuscript include the following:

Tables S1 to S3.

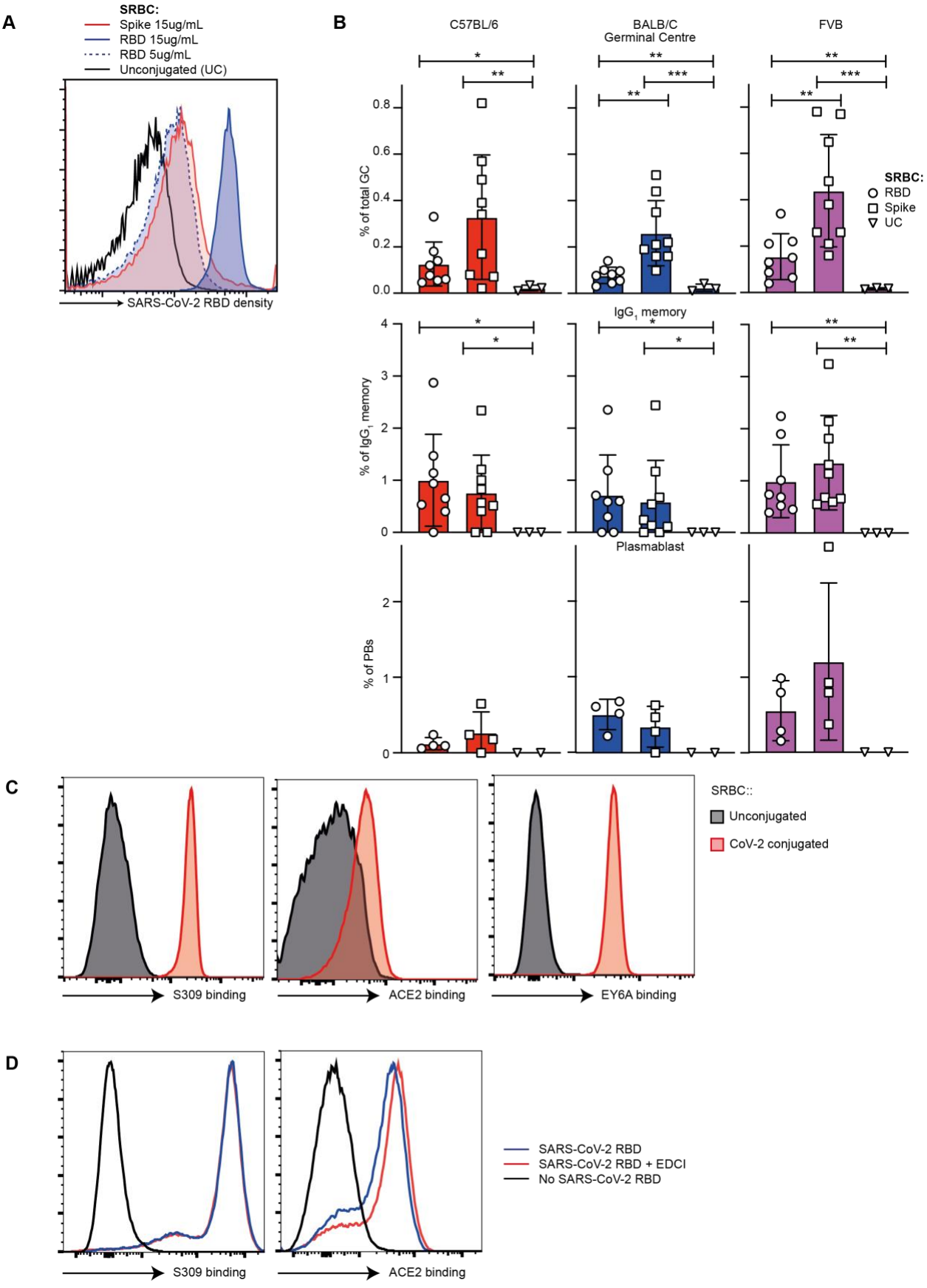
A
SRBC:
Spike 15ug/mL
RBD 15ug/mL
RBD 5ug/mL
Unconjugated (UC)
SARS-CoV-2 RBD density
B
C57BL/6
BALB/C
Germinal Centre
FVB
% of total GC
SRBC:
RBD
Spike
UC
IgG1 memory
% of IgG1 memory
Plasmablast
% of PBs
C
SRBC::
Unconjugated
CoV-2 conjugated
S309 binding
ACE2 binding
EY6A binding
D
SARS-CoV-2 RBD
SARS-CoV-2 RBD + EDCI
No SARS-CoV-2 RBD
S309 binding
ACE2 binding

Figure S1. Validation of experimental model (refers to figure 1)

A. Relative density of SARS-CoV-2 Spike (red) or RBD (blue) on sheep red blood cells (SRBCs) conjugated at 15ug/mL (solid line) or 5ug/mL (dashed line).
B. Mice of the indicated strains were immunized with RBD-SRBCs (conjugated at 5ug/ml), Spike-SRBC or unconjugated SRBCs (UC) and spleen cells analyzed 7 days later to measure the percentage of GC B cells (B220+, Fas+, CD38-, top panel), IgG1 memory cells (B220+, Fas-, IgG1+, middle panel) or plasmablasts (B220low, TACI+, CD138+, bottom panel) binding fluorescent tetramers of SARS-CoV-2 RBD .

Data points represent one mouse. Data pooled from 2 independent experiments.

C. Binding of EY6A, S309 or ACE2Fc to SRBC conjugated with 10ug/mL SARS-CoV-2 RBD (red) or unconjugated SRBC (black).
D. Binding of S309 or ACE2Fc to EDCI conjugated (red) or unconjugated SARS-CoV-2 RBD incubated at 2ug/mL on CR3022 knock-in mouse B cells.

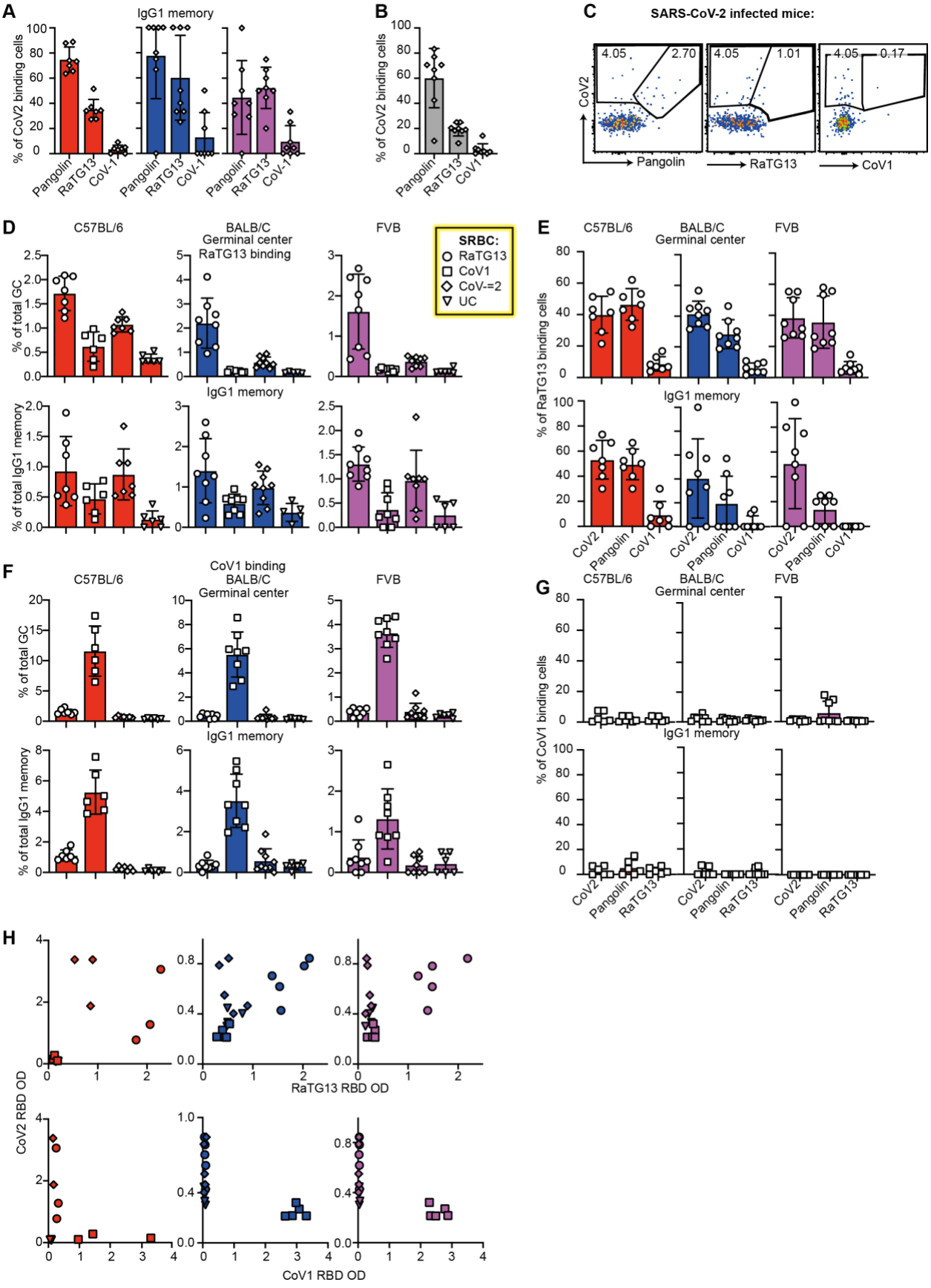
A
IgG1 memory
% of CoV2 binding cells
Pangolin
RaTG13
CoV-1
B
% of CoV2 binding cells
CoV1
C
SARS-CoV-2 infected mice:
CoV2
4.05
2.70
1.01
0.17
Pangolin
RaTG13
CoV1
D
C57BL/6
BALB/C
Germinal center
FVB
RaTG13 binding
IgG1 memory
% of total GC
% of total IgG1 memory
SRBC:
RaTG13
CoV1
CoV-=2
UC
E
% of RaTG13 binding cells
CoV2
F
CoV1 binding
% of total GC
% of total IgG1 memory
G
% of CoV1 binding cells
H
RaTG13 RBD OD
CoV2 RBD OD
CoV1 RBD OD

Figure S2. B cell response elicited by RBD-focused immunization included broadly cross-reactive cells in standard inbred lines (refers to figure 1)

E. Cross-reactivity of the CoV2 binding IgG1 memory response to pangolin, RaTG13 and CoV1 in C57BL/6 (red), BALB/C (blue) and FVB (purple) strains of mice 7 days following immunization with CoV2 conjugated SRBCs.

F. Cross-reactivity of the SARS-CoV-2 binding germinal center response of C57BL/6 mice with humanized ACE2 receptors, infected with 1 x 10^4 PFU SARS-CoV-2 on days 5-6.

G. Representative flow cytometric plots illustrating the antigen specific tetramer strains in the SARS-CoV-2 infections.

H. Proportion of the total GC or IgG1 memory response binding to RaTG13 tetramers following immunization of C57BL/6 (red), BALB/C (blue) and FVB (purple) mice with RaTG13 (circles), CoV1 (squares), CoV2 (diamonds) RBD or unconjugated SRBCs (triangles) one week prior.

I. Cross-reactivity of the RaTG13 binding germinal center and IgG1 memory response to pangolin, RaTG13 and CoV1 RBD in mice 7 days following immunization with RaTG13 conjugated SRBC.

J. Proportion of the total GC or IgG1 memory response binding to CoV1 RBD tetramers following immunization of C57BL/6 (red), BALB/C (blue) and FVB (purple) mice with RaTG13 (circles), CoV1 (squares), CoV2 (diamonds) RBD or unconjugated SRBCs (triangles) one week prior.

K. Cross-reactivity of the CoV1 binding germinal center and IgG1 memory response to pangolin, RaTG13 and CoV2 RBD in mice 7 days following immunization with CoV1 conjugated SRBC.

L. ELISAS from C57BL/6 (red), BALB/C (blue), FVB (purple) mice immunized with RaTG13 (circles), CoV1 (squares), CoV2 (diamonds) RBD or unconjugated SRBCs (triangles) one week prior showing optical density (OD) of serum IgK antibodies binding to CoV2 RBD (Y axis), RaTG13 RBD (X axis top panel), or CoV1 RBD (X axis bottom panel).
Data points represent one mouse. Data pooled from 2 independent experiments.

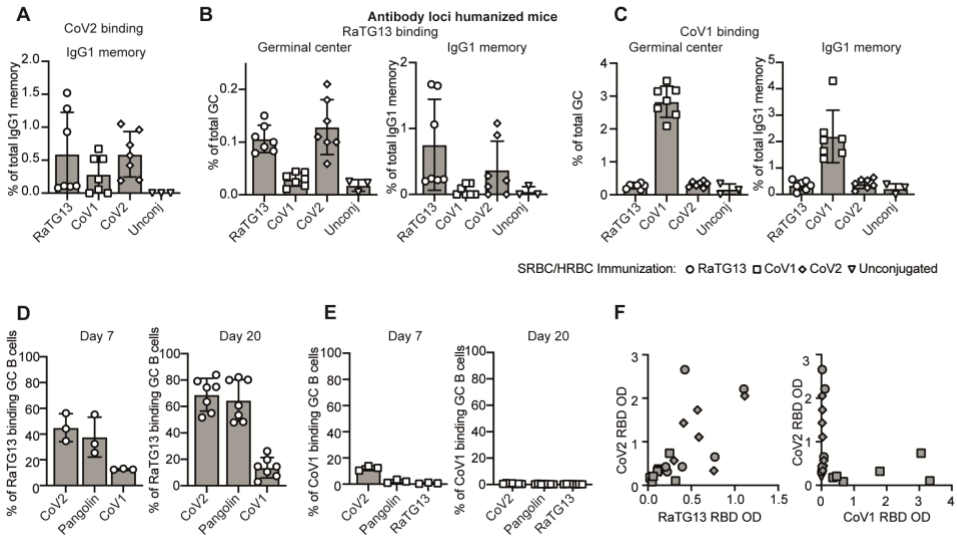

Figure S3. B cell response elicited by RBD-focused immunization included broadly cross-reactive cells in Ig-humanized mice (refers to figure 1)

A-C. Proportion of the total IgG1 memory response binding to CoV2 (A), RaTG13 (B) or CoV1(C) RBD tetramers following immunization of humanized V-gene mice with RaTG13 (circles), CoV1 (squares), CoV2 (diamonds) RBD or unconjugated (triangles) SRBCs one week prior.

D-E. Cross-reactivity of the RaTG13 (D) or CoV1 (right) binding GC response in humanized mice 7 (left) or 20 (right) days following immunization with RaTG13 (D) or CoV1 (E) conjugated SRBCs/HRBCs.

F. ELISAS from humanized mice immunized with RaTG13 (circles), SARS-CoV-1 (squares), SARS-CoV-2 (diamonds) RBD or unconjugated SRBCs (triangles) one week prior showing optical density (OD) or serum IgK antibodies binding to CoV2 (Y axis), RaTG13 (X axis top panel), or CoV1 RBD (X axis bottom panel).

Data points represent one mouse or individual. Data in A-G pooled from 2 independent experiments.

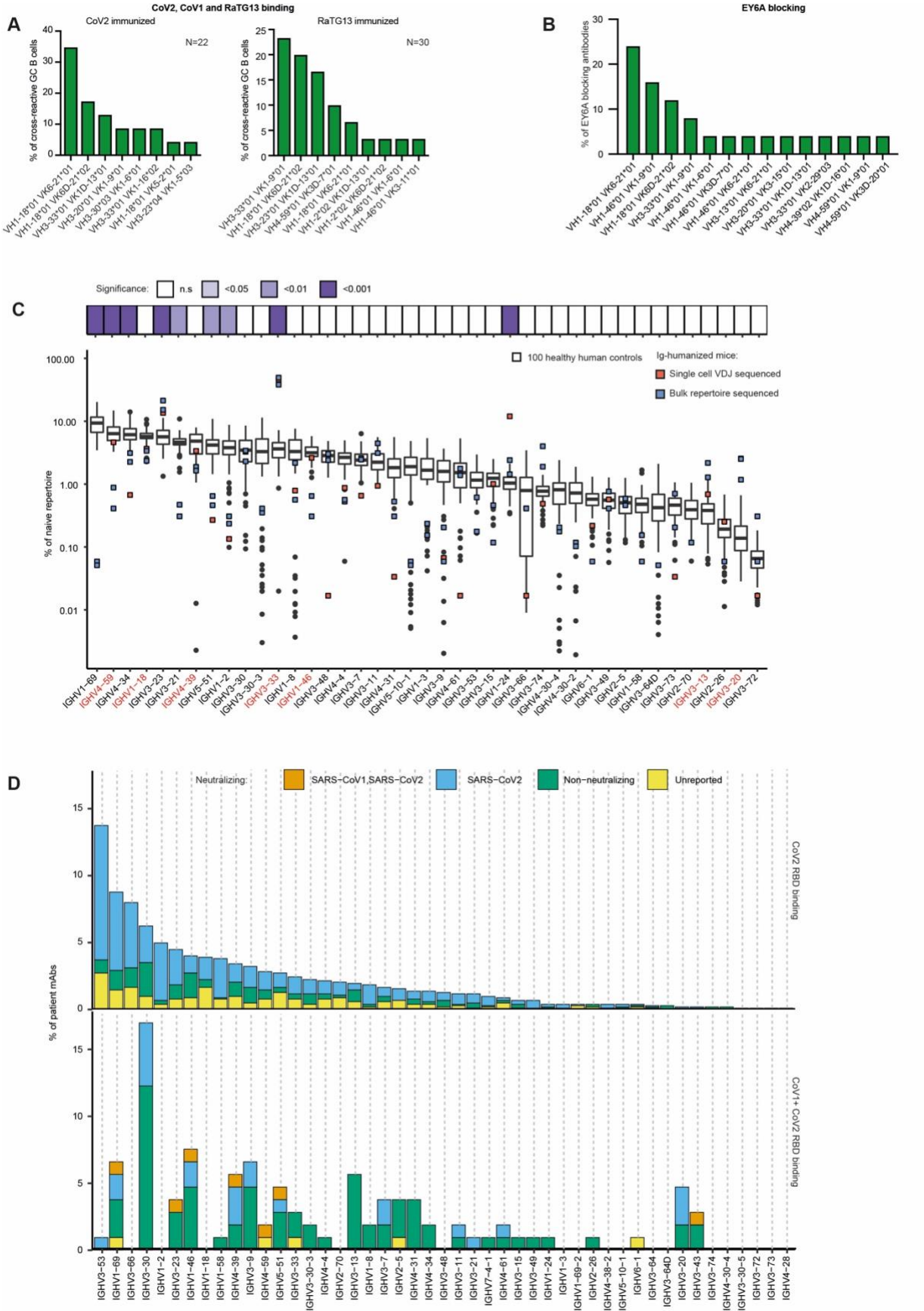
A
CoV2, CoV1 and RaTG13 binding
CoV2 immunized
N=22
% of cross-reactive GC B cells
VH1-18*01 VK6-21*01
VH1-18*01 VK6D-21*02
VH3-33*01 VK1D-13*01
VH3-20*01 VK1-9*01
VH3-30*03 VK1-6*01
VH3-33*01 VK1-16*02
VH1-18*01 VK5-2*01
VH3-23*04 VK1-5*03
RaTG13 immunized
N=30
% of cross-reactive GC B cells
VH3-33*01 VK1-9*01
VH1-18*01 VK6D-21*02
VH3-23*01 VK1D-13*01
VH4-59*01 VK3D-7*01
VH1-18*01 VK6-21*01
VH1-2*02 VK1D-13*01
VH1-2*02 VK6D-21*02
VH1-46*01 VK1-6*01
VH1-46*01 VK3-11*01
B
EY6A blocking
% of EY6A blocking antibodies
VH1-18*01 VK6-21*01
VH1-46*01 VK1-9*01
VH1-18*01 VK6D-21*02
VH3-33*01 VK1-9*01
VH1-46*01 VK1-6*01
VH1-46*01 VK3D-7*01
VH1-46*01 VK6-21*01
VH3-13*01 VK6-21*01
VH3-20*01 VK3-15*01
VH3-33*01 VK1D-13*01
VH3-33*01 VK2-29*03
VH4-39*02 VK1D-16*01
VH4-59*01 VK1-9*01
VH4-59*01 VK3D-20*01
C
Significance: n.s <0.05 <0.01 <0.001
100 healthy human controls
Ig-humanized mice:
Single cell VDJ sequenced
Bulk repertoire sequenced
% of naive repertoire
IGHV1-69 IGHV4-59 IGHV4-34 IGHV1-18 IGHV3-23 IGHV3-21 IGHV4-39 IGHV5-51 IGHV1-2 IGHV3-30 IGHV3-30-3 IGHV3-33 IGHV1-8 IGHV1-46 IGHV3-48 IGHV4-4 IGHV3-7 IGHV3-11 IGHV4-31 IGHV5-10-1 IGHV1-3 IGHV3-9 IGHV4-61 IGHV3-53 IGHV3-15 IGHV1-24 IGHV3-66 IGHV3-74 IGHV4-30-4 IGHV4-30-2 IGHV6-1 IGHV3-49 IGHV2-5 IGHV1-58 IGHV3-64D IGHV3-73 IGHV2-70 IGHV3-13 IGHV2-26 IGHV3-20 IGHV3-72
D
Neutralizing: SARS-CoV1,SARS-CoV2 SARS-CoV2 Non-neutralizing Unreported
% of patient mAbs
CoV2 RBD binding
CoV1+ CoV2 RBD binding
IGHV3-53 IGHV1-69 IGHV3-66 IGHV3-30 IGHV1-2 IGHV3-23 IGHV1-46 IGHV1-18 IGHV1-58 IGHV4-39 IGHV3-9 IGHV4-59 IGHV5-51 IGHV3-33 IGHV3-30-3 IGHV4-4 IGHV2-70 IGHV3-13 IGHV1-8 IGHV3-7 IGHV2-5 IGHV4-31 IGHV4-34 IGHV3-48 IGHV3-11 IGHV3-21 IGHV7-4-1 IGHV4-61 IGHV3-15 IGHV3-49 IGHV1-24 IGHV1-3 IGHV1-69-2 IGHV2-26 IGHV4-38-2 IGHV5-10-1 IGHV6-1 IGHV3-64 IGHV3-64D IGHV3-20 IGHV3-43 IGHV3-74 IGHV4-30-4 IGHV3-30-5 IGHV3-72 IGHV3-73 IGHV4-28

Figure S4. B cell response to coronavirus RBDs in Ig-humanized mice included recurrent *IGHV/IGKV* pairs (refers to figure 3 and figure 4)

A. *IGHV/IGKV* use as a % of total single cell sorted GC B cells triple-binding to CoV2, CoV1 and RaTG13 RBD tetramers, from humanized immunoglobulin repertoire mice following 20 days of immunizations with SARS-CoV-2 or RaTG13 RBD. Number of sequenced cells is indicated in the top right of each graph.

B. *IGHV/IGKV* used by antibodies that blocked fluorescently tagged EY6A from binding CoV2 RBD more effectively than CR3022.

C. *IGHV* usage in naive B cells (IgM, unmutated) from 100 healthy human controls (data obtained from BioProject PRJNA491287) compared to single cell sequenced (red) or bulk repertoire sequenced (blue) naïve IgM B cells from 3 unimmunized Ig-humanized mice. *IGHV* regions that represented the class 4 cross-reactive antibodies in B are indicated in red.

Adjusted P values for comparing *IGHV* region frequency between naïve human and mouse repertoires, as assessed by ANOVA and Tukey HSD post-test, are indicated in the tiles at the top of the panel.

D. *IGHV* usage by RBD-binding antibodies in CoV-AbDab isolated from SARS-CoV-2 infected people and found to bind CoV2 but not CoV1 (top) or bind CoV2 and CoV1 (bottom). Note the paucity of *IGHV3-53* and *IGHV3-66* antibodies among CoV1/CoV2 cross-reactive antibodies compared to CoV2-only antibodies. Antibodies tested for neutralizing activity against one or both viruses are denoted by colors in the key.

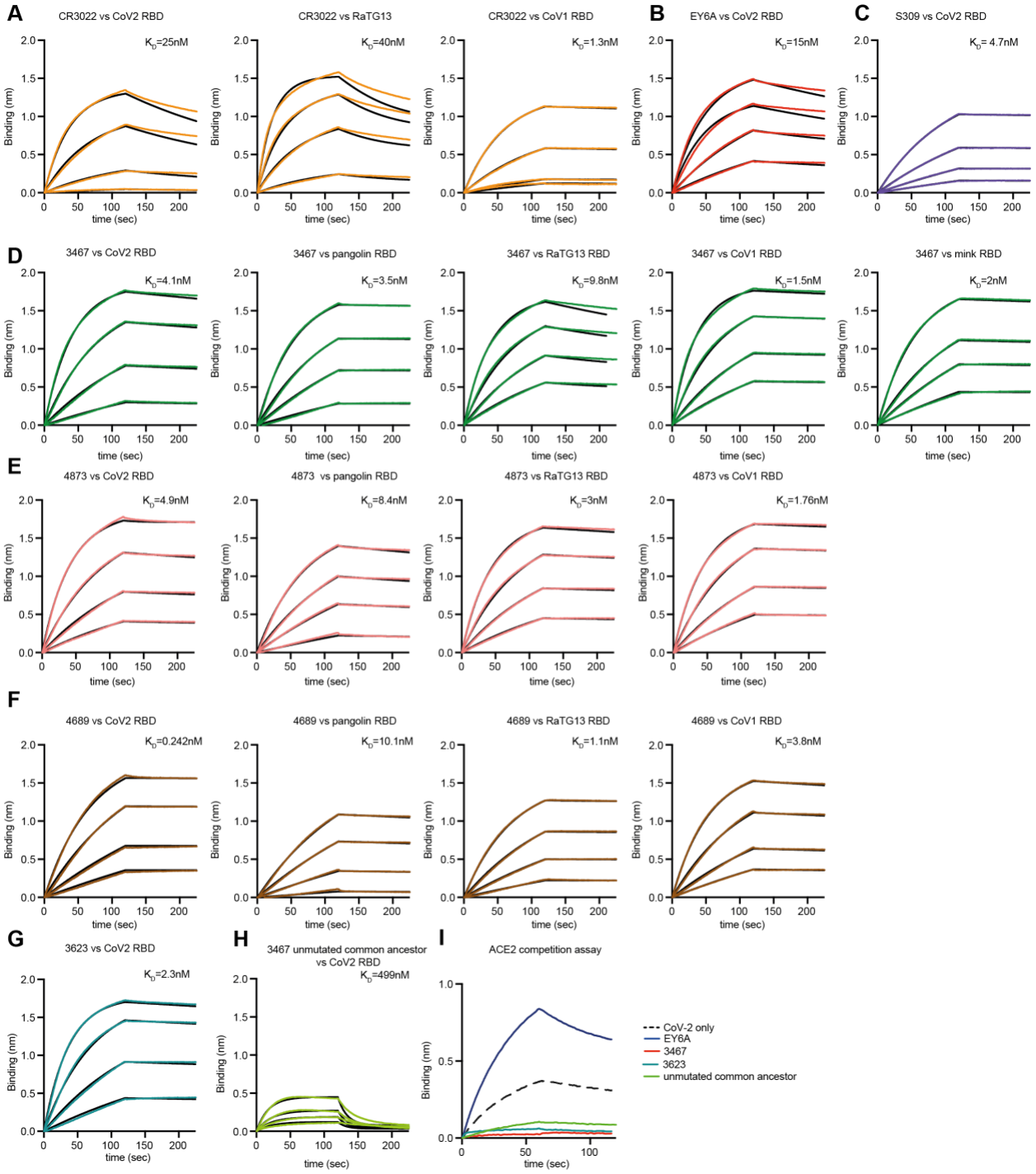

Figure S5. Binding, affinity and epitope specificity of antibodies to diverse sarbecovirus RBDs (refers to figure 5).

A-H. Association and dissociation of soluble protein binding to the indicated RBD antigens to biotinylated humanized IgG1 antibodies immobilized onto streptavidin biosensors, as measured by bio-layer interferometry.

I. biotinylated ACE2-Fc was immobilized onto streptavidin sensors and incubated with either CoV2 RBD at 500nM alone or following pre-incubated with the indicated IgG1 at 1 μM.

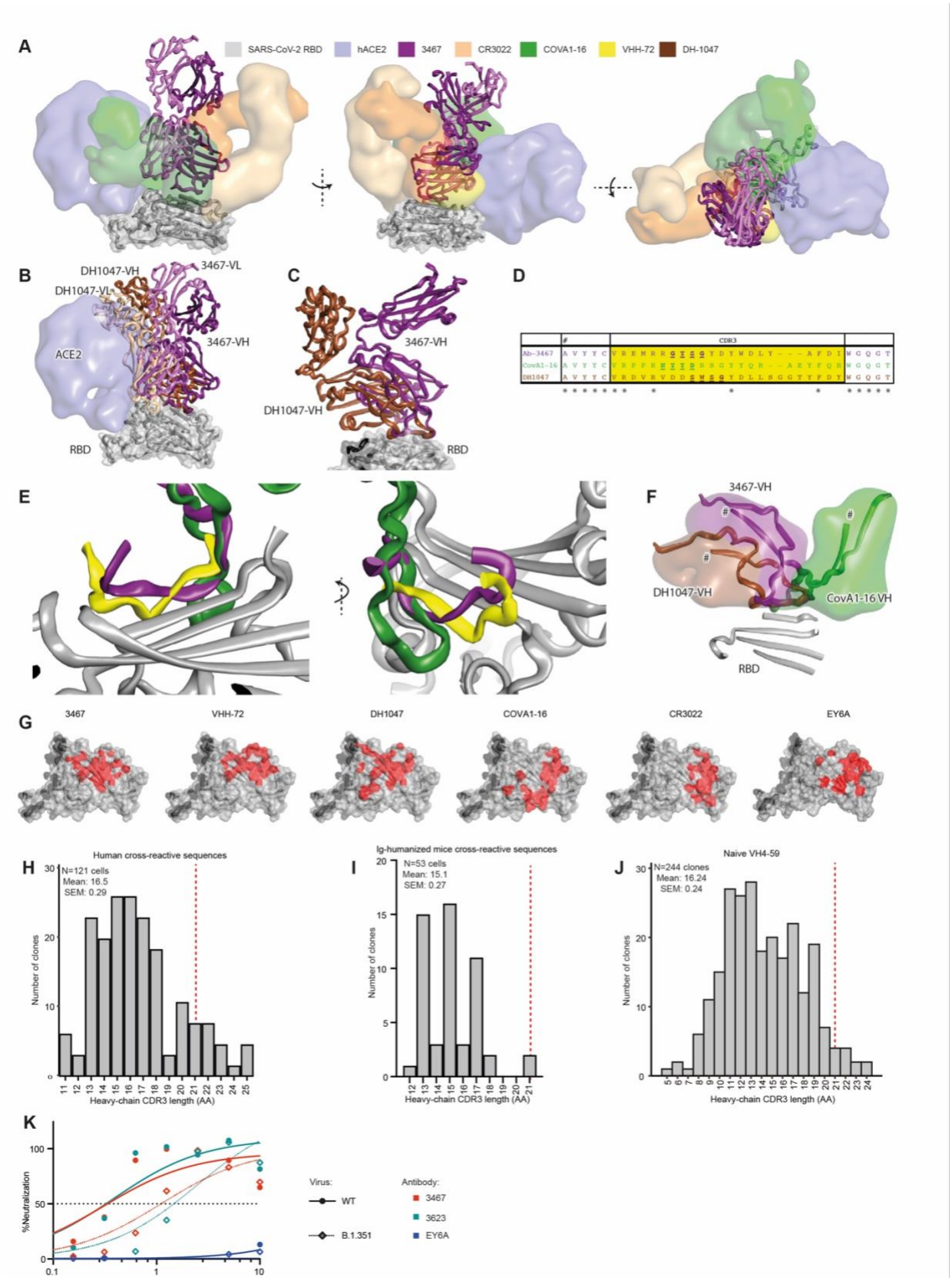
A
SARS-CoV-2 RBD
hACE2
3467
CR3022
COVA1-16
VHH-72
DH-1047
B
DH1047-VH
DH1047-VL
3467-VL
3467-VH
ACE2
RBD
C
3467-VH
DH1047-VH
RBD
D
CDR3
Ab-3467
CovA1-16
DH1047
E
F
3467-VH
DH1047-VH
CovA1-16 VH
RBD
G
3467
VHH-72
DH1047
COVA1-16
CR3022
EY6A
H
Human cross-reactive sequences
N=121 cells
Mean: 16.5
SEM: 0.29
Number of clones
Heavy-chain CDR3 length (AA)
I
Ig-humanized mice cross-reactive sequences
N=53 cells
Mean: 15.1
SEM: 0.27
Number of clones
Heavy-chain CDR3 length (AA)
J
Naive VH4-59
N=244 clones
Mean: 16.24
SEM: 0.24
Number of clones
Heavy-chain CDR3 length (AA)
K
%Neutralization
Virus:
WT
B.1.351
Antibody:
3467
3623
EY6A

Figure S6. Features of class 4 antibodies that facilitated neutralization (refers to figure 6 and figure 7)

A. Crystal structure AB-3467 Fab (heavy and light chains as dark and light purple cartoons) with the SARS-CoV-2 RBD (grey surface and cartoon). The surfaces for antibody CR3022 (shades of orange), COVA1-16 (shades of green), VHH-72 (shades of yellow) and hACE2 (shades of blue) are overlaid as reference controls. Three perspectives are shown.
B. Structure and positioning of AB-3467 Fab (heavy and light chains as dark and light purple cartoons) compared to DH1047 (heavy and light chains as dark and light brown cartoons).
C. Comparison of the structure and positioning of AB-3467 (purple) and DH1047 (brown) heavy chain on the RBD. The ACE2 binding interface on the RBD is indicated in black.
D. Comparison of the heavy chain CDR3 of AB-3467, CovA1-16 and DH1047. Underlined residues indicate those that extend the RBD beta sheet.
E. Two different perspectives showing comparing the abilities of AB-3467 (purple), COVA1-16 (green) and VHH-72 (yellow) to extend the RBD (grey) beta-sheet.
F. The heavy chain VH domain for AB-3467 (purple), CovA1-16 (green) and DH1047 (brown) extending the beta sheet of the RBD beginning at the # residues indicated in D.
G. Contact residues on the surface of the RBD (red) for the indicated antibodies. The ACE2 binding surface is also indicated in black for reference.
H. Distribution of CDRH3 lengths from sorted memory cells from human convalescent patients cross-reactive to CoV2, CoV1 and RaTG13.
I. Distribution of CDRH3 lengths from sorted GC cells from humanized Ig mice immunized with CoV2 or RaTG13 RBD cross-reactive to CoV2, CoV1 and RaTG13.
J. Distribution of CDRH3 lengths from clones expressing the VH4-59 heavy chain sequenced from a naïve humanized antibody loci mouse. The relative position AB-3467 would lie on this graph is indicated by a red dashed line.
K. Cytopathic effect of intact virus neutralization in vero cells for antibody 3467, 3623 and EY6A against the POWO7 (WT) and B.1.351 strains of the virus.

Table S1. Sequence identity and binding residues of neutralizing class 4 antibodies (refers to figures 3 and 5).

A. Amino acid conservation across the RBD for divergent sarbecovirus lineages. The entropy score for each residue of the RBD across 192,000 coronavirus genomes is indicated. Heavy and light chain contact residues are indicated for the listed antibodies.

B. Full details of all BCR sequences with the *VH4-59 VK1-9 IGH/IGK* isolated from human V-gene transgenic mice following 20 days of immunization with CoV1 RBD SRBC and HRBC. Sequences in black text are those isolated from B cells that also bound CoV1 and CoV2 tetramers, while those in red bound CoV1 tetramers only. Those highlighted in yellow indicate those sequences that were expressed for further analysis. Contact residue sites of antibody 3467 with the CoV2 RBD are indicated by an asterisk.

Table S2. Sarbecovirus RBD binding B cells sequenced from humans and mice (refers to figure 3, figure 4 and figure 5).

A-C. Details of the total single cell B cell receptor sequences of RBD antigen binding germinal center B cells elicited from human V-gene transgenic mice following 20 days of immunization with CoV2 (A), CoV1(B) or RaTG13 RBD (C).

A. Details of the total single cell B cell receptor sequences of CoV1, CoV2 and RaTG13 RBD antigen binding GC B cells elicited from human V-gene transgenic mice following 20 days of immunization with CoV2 or RaTG13 RBD SRBC and HRBC.

E-G. Details of the total single cell B cell receptor sequences of CoV1, CoV2 and RaTG13 RBD antigen binding GC B cells elicited from human V-gene transgenic mice 7 days following a single immunization with CoV2 (E), CoV1 (F) or RaTG13 (G) RBD SRBC.

L. Details of the total single cell B cell receptor sequences of CoV1, CoV2 and RaTG13 RBD antigen binding IgD- memory cells isolated from two human convalescent patients 4 months following natural infection.

Table S3. Binding data of expressed antibodies (refers to figure 5).

A. Details of all antibodies expressed in this study, including their full sequence, the sorting strategy used to isolate them, the IgK MFI of their binding to CoV2 Spike, CoV2 RBD, CoV1 RBD, RaTG13 RBD and Mink RBD conjugated SRBC at 10ug/mL and the IgK MFI of fluorescently labelled EY6A, S309, P2B-2F6 or ACE2FC binding to CoV2 RBD conjugated SRBC, following the addition of 10ug/mL of each of the indicated antibodies. Antibodies indicated in red are those that bound to CoV2, CoV1 and RaTG13. Antibodies highlighted in yellow are previously published antibodies described by other studies.

B. Details of all *VH4-59 VK1-9* antibodies expressed in this study including the IgK MFI of their of binding to CoV2 Spike, CoV2 RBD, CoV1 RBD, RaTG13 RBD and Mink RBD conjugated SRBC at 10ug/mL and the IgK MFI of fluorescently labelled EY6A, binding to CoV2 RBD conjugated SRBC, following the addition of 10ug/mL of each of the indicated antibodies.

X-Ray Diffraction Data Collection Statistics	
Crystal	**AB-3467 Fab + CoV-2 RBD**
Wavelength	0.9537
Spacegroup	$C222_1$
Unit cell dimensions: a, b, c (Å); *α, β, γ*, (°)	109.76, 115.49, 240.76; *90.00, 90.00, 90.00*
Resolution range	2.29-48.15 (2.29-2.35)
Total reflections	938116 (59880)
Unique reflections	68595 (4460)
Completeness	99.8 (97.5)
Multiplicity	13.7 (13.4)
Average (I/σ(I))	22.5 (4.0)
Mean half set correlation, $CC_{1/2}$	0.999 (0.882)
Rmeas (all I+ and I-)	0.078 (0.776)
Rpim (all I+ and I-)	0.021 (0.208)
Wilson B (Å^2)	44.4
Refinement and Model Statistics	
R_{work}/R_{free}	0.204/0.256
Proteins/asu	2 x AB-3467 Fab, 2 x CoV-2 RBD
Atoms protein	9456
B average protein (Å^2)	52.1
B average molecule (Å^2)	RBD chain A; 63.2 RBD chain B; 62.3 AB-3467 heavy chain H; 46.7 AB-3467 light chain L; 48.6 AB-3467 heavy chain D; 47.4 AB-3467 light chain E; 46.6
Carbohydrate	Chain A, Asn343 linked; 2 x NAG, 1 x FUC, 1 x MBA ,1 x MAN
B average carbohydrate (Å^2)	80.3
Waters	164
B average water (Å^2)	42.7
RMSD bond lengths (Å)	0.0085
RMSD bond angles (°)	1.57
Ramachandran Outliers (%)	0.57
Ramachandran Favored (%)	91.6
PDB entry	**7msq**

Table S4. X-Ray Diffraction Data Collection Statistics (refers to figure 6)

Diffraction data and model refinement statistics. Values in parentheses represent values for the highest resolution shell.